Chapter 4

Comparison of CapZ Subunits and Analysis of the *sne* Phenotype

Chapter 4: Comparison of CapZ subunits and analysis of the *sne* phenotype

4.1 Summary

In the previous chapter the positional cloning of the *sne* locus to *capzα1* was described. In the first part of this chapter I primarily focus on comparing the homology of the known zebrafish CapZ subunits (CapZα1, CapZα2 and CapZβ) to other species. These homology comparisons confirm that the site of the mutation is indeed in *capzα1*. Moreover, they illustrate how extremely well conserved the CapZ subunits are across vertebrates. Analysis of the temporal and spatial expression pattern of the CapZ subunits reveals that all subunits are maternally expressed and are ubiquitous in the early stages of zebrafish development. However, by 24 hpf the *capzα2* expression pattern differs to that of *capzα1* and *capzβ*. These findings could reflect a situation in which the α subunits are partially redundant during early development, but take on specific/unique roles during muscle differentiation. The final section of this chapter describes the *sne* mutant phenotype. In *sne* mutants wavy skeletal myofibres and reduced motility are observed from 4 days post fertilization (dpf). Intriguingly, the expression of *capzα1* itself is not affected in the mutants, and immunostaining of CapZα1 reveals that mutant forms of CapZα1 are translated, albeit with an altered cellular localization. In wild type skeletal muscle, CapZα1 is detected at the Z-line, however in *sne* mutant embryos aggregates of protein are observed adjacent to the myoseptum boundaries. Further immunostaining of sarcomeric components and transmission electron microscopy (TEM) analysis indicate that although the main elements that define the sarcomere are still preserved, the mutation in *capzα1* disrupts myofibrillar organization and sarcomeric integrity. Indeed, the muscle phenotype worsens over time in *sne* mutant embryos and when the movements of mutant embryos are restricted, the skeletal muscle phenotype is partially

rescued. These findings provide further support for the prediction that the mutation in *capzα1* destabilizes skeletal muscle architecture following the commencement of contraction.

4.2 Introduction

CapZ is a heterodimeric capping protein that consists of α and β subunits that dimerize to form a fully functional protein, which caps the barbed end of actin filaments. Expression studies performed in yeast, *Dictyostelium* and in cultured vertebrate muscle cells indicate that CapZ is only stable as a heterodimer, and that the individual subunits are highly unstable and have little or no function *in vivo* or *in vitro* (Amatruda et al., 1992; Hug et al., 1995; Hug et al., 1992; Schafer et al., 1992). Invertebrates such as *C. elegans* or *D. melanogaster* express only one of each of the CapZ α and β subunits, however, up to three different α and β isoforms have been found in vertebrates. The production of distinct isoforms is achieved in different ways; the α subunits are encoded on separate genes, while the β subunits are produced from alternative splicing of one transcript. Two isoforms of CapZ α (CapZα1 and CapZα2) and β (CapZβ1 and CapZβ2) exist in chicken, mouse and human (Hart et al., 1997b). In mammals, a third isoform of the α and β subunits (*capZα3* and *capZβ3*) have also been found and are only expressed in male germ cells (Hart et al., 1997a; Schafer et al., 1994; von Bulow et al., 1997).

To date, research on CapZ has focused on how it controls actin dynamics *in vitro* and relatively little is known about potential alternate roles of CapZ in vertebrate development. Indeed, the high homology shared between the CapZ subunits of different species and their early expression during development suggest that they are essential components for vertebrate development and function.

4.3 Comparison of CapZ subunit sequences between species

4.3.1 CapZα1 and CapZα2

In zebrafish only two isoforms of *capZα* (*capZα1* and *capZα2*) were identified and they are located on chromosomes 8 and 6 respectively. CapZα1 and CapZα2 are highly conserved between species and over 80% amino acid sequence identity was observed when zebrafish CapZα1 and CapZα2 were aligned with chicken, mouse, and human orthologues (Fig. 4.1 and Fig. 4.2). Intriguingly, not only are both these proteins the same length (286 residues) but they also share 86 % sequence identity in zebrafish. A similar percentage was also observed between CapZα1 and CapZα2 in the other vertebrates that were compared (Fig. 4.3). CapZα1 and CapZα2 are so highly conserved within vertebrates that the regions between 23 -58 amino acids and 239-286 amino acids are invariant between zebrafish, chicken, mouse and human. The C-terminal region (239-286 amino acids) is thought to be important for actin binding (Casella and Torres, 1994; Hug et al., 1992; Sizonenko et al., 1996). Notably, the mutation identified at the splice junction in *sne* affects translation of the C-terminal region.

One of the major discrepancies caused by the high similarity between *capzα1* and *capzα2* became apparent in Ensembl. In the latest version of the zebrafish genome assembly (Zv6) the *capzα* gene on chromosome 6 is assigned *capzα1* while the *capzα* gene on chromosome 8 (*sne* locus) is assigned as an 'unknown' gene. As described below, I have used different sequence comparison tools to analyze orthologues of the different CapZ subunits, to verify that the gene on chromosome 8 is in fact *capzα1*, and the gene on chromosome 6 is *capzα2*. For the remainder of this thesis zebrafish *capzα1* will always refer to the gene encoded on chromosome 8 and *capzα2* will refer to the gene on chromosome 6.

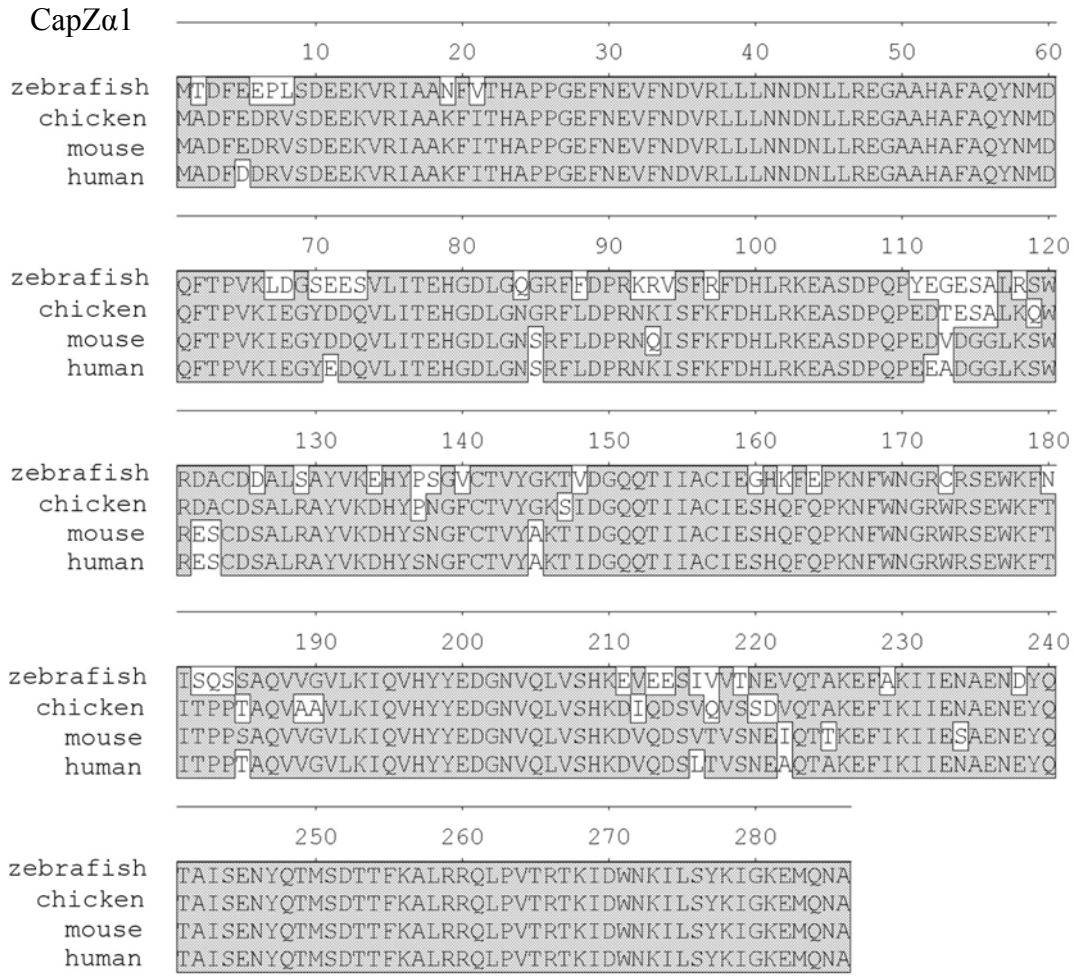

Fig. 4.1. Alignment of zebrafish, chicken, mouse and human CapZα1 protein sequence.

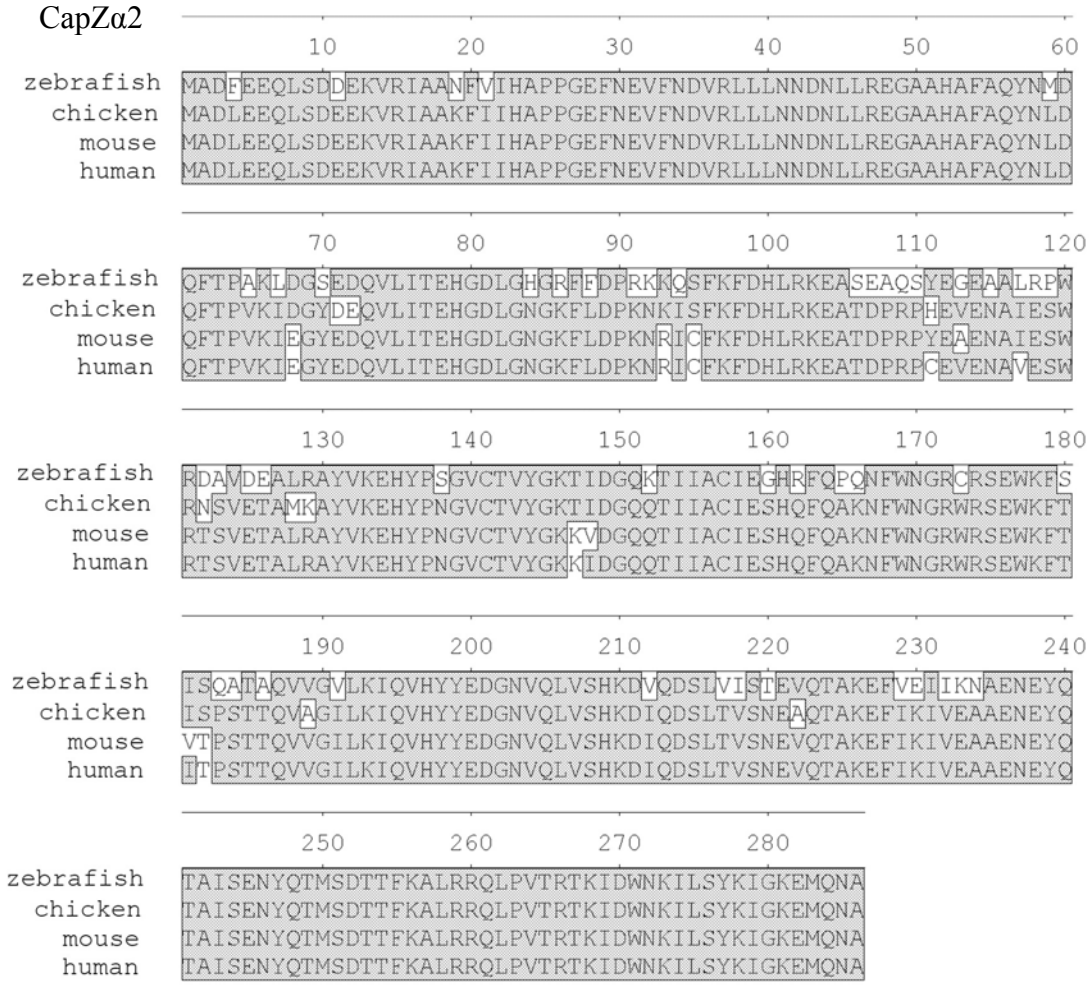

Fig. 4.2. Alignment of zebrafish, chicken, mouse and human CapZα2 protein sequence.

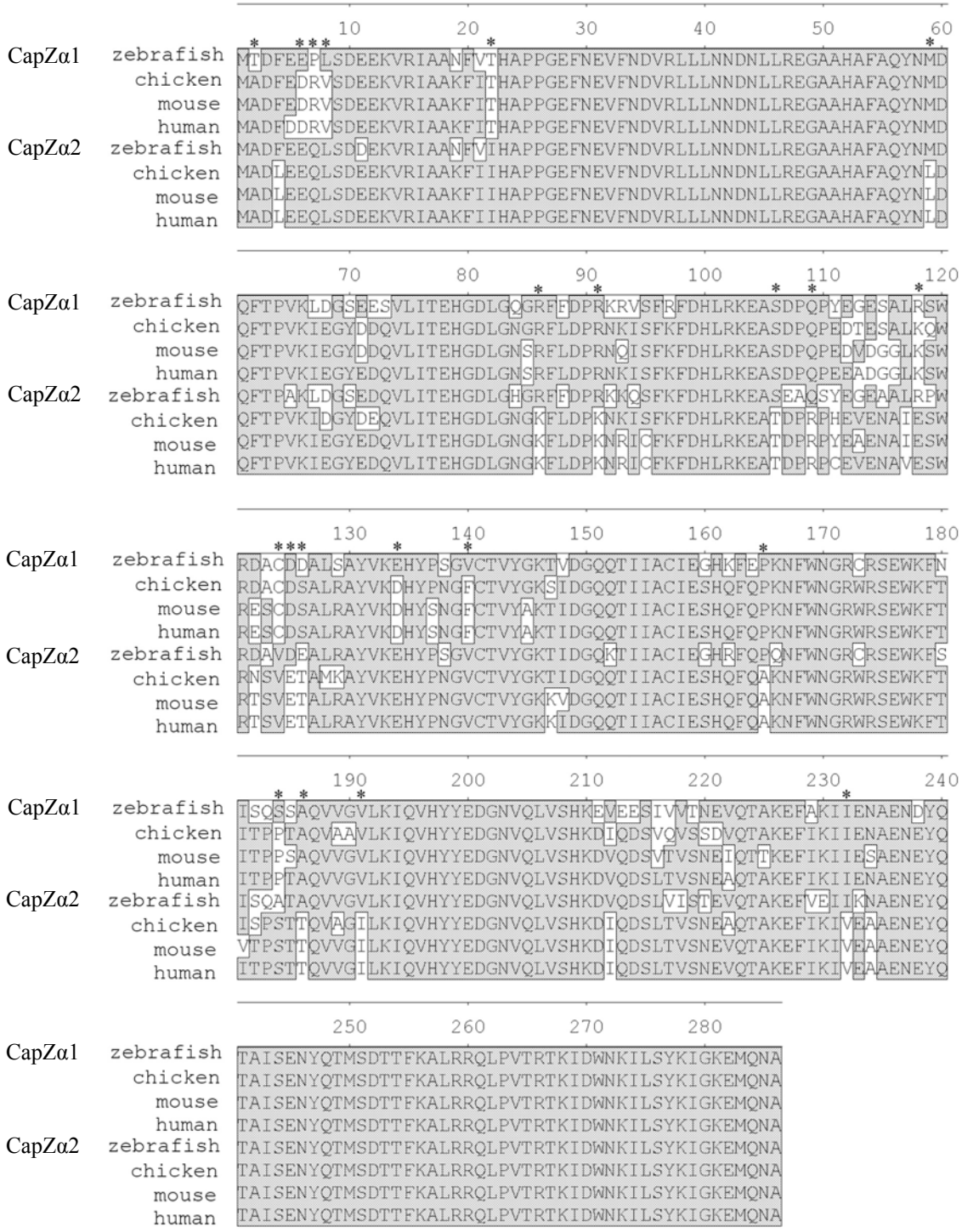

Fig. 4.3. Alignment of CapZα1 and CapZα2 protein sequence from zebrafish, chicken, mouse and human. Amino acids that are identical between the majority of orthologues are shaded. Asterisks indicate residues that are distinctive between CapZα1 and CapZα2 in chicken, mouse and human as determined by Hart et al. 1997b. The percentage identities shared between CapZα1 and CapZα2 of zebrafish, chicken, mouse and human are 86%, 85%, 84% and 86% respectively.

A phylogenetic tree was initially generated using CapZα1 and CapZα2 protein sequences, aligned by Clustal W, to determine whether the two zebrafish isoforms clustered with CapZα1 and CapZα2 sequence of the higher vertebrates (Fig. 4.4A). The tree groups the CapZα1 and CapZα2 sequences of mouse, chicken and human separately, however, zebrafish CapZα1 and CapZα2 were clustered with the CapZα1subunits of other fish species. It is therefore impossible to ascertain whether zebrafish CapZα1 is orthologous to CapZα1 or CapZα2 in the higher vertebrates using these alignment parameters. Interestingly, both medaka and stickleback have two CapZα1 subunits. Moreover, the α2 subunits from these species clustered with the α2 subunits of higher vertebrates. It could be speculated that zebrafish CapZα1 may in fact be CapZα1b, however, no other gene of the CapZα family has been identified in the zebrafish genome. As DNA sequence is generally not as well conserved as protein sequence another phylogenetic tree was generated using *capzα1* and *capzα2* cDNA sequence (Fig. 4.5). Strikingly, similar clusters were observed as in the protein phylogenetic tree, emphasizing the high level of α subunit conservation across species.

A comparison study of the CapZα1 and CapZα2 isoforms performed by Hart and colleagues (1997b) claimed to identify key amino acid differences between CapZα1 and CapZα2. They identified 21 residues that demonstrated isoform specificity when the two isoforms of chicken, mouse and human were aligned (asterisks in Fig. 4.3). To determine whether this isoform specificity was also conserved in zebrafish and could be used to distinguish the two α subunits, these key residues were examined. Unfortunately in zebrafish, only two out of the 21 residues were isoform specific for CapZα1 and CapZα2, and also matched the amino acid residues in the respective orthologues (amino acid 22 and amino acid 124). The majority of the key residues were identical between CapZα1 and CapZα2 in zebrafish (16/21). The remaining three key residues differed between the two zebrafish isoforms, however, did not match the

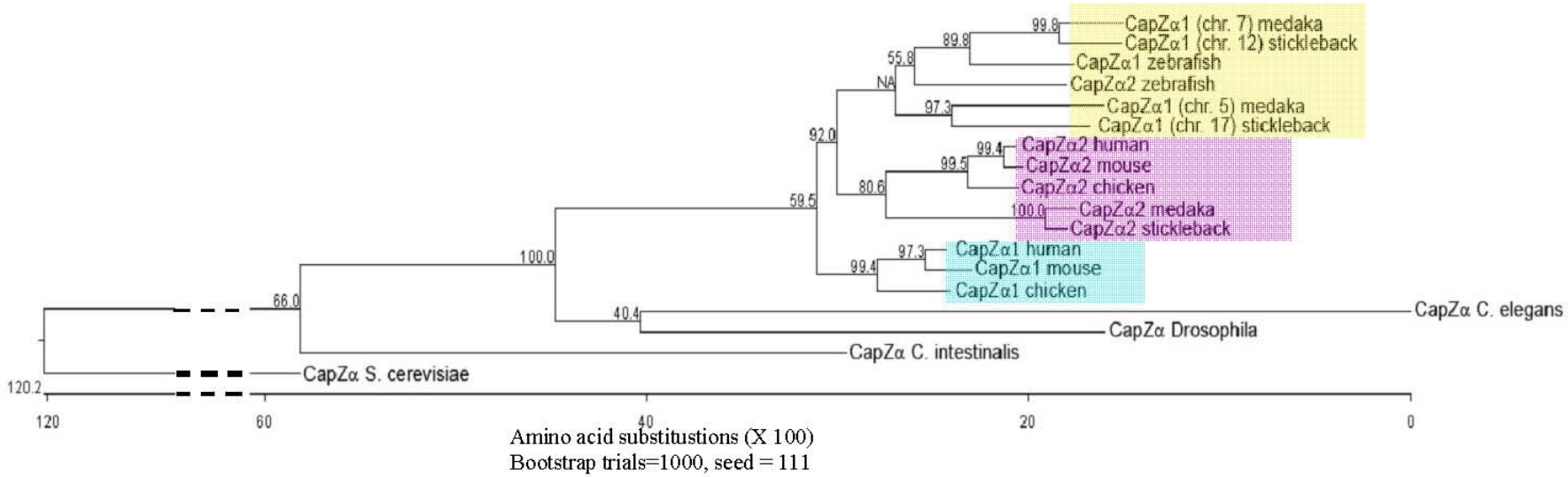

Fig.4.4A. Phylogenetic tree of CapZα subunits from various species. The Clustal W program was used to align amino acid sequences from yeast (*S. cerevisiae*), worm (*C. elegans*), *Drosophila*, *C. intestinalis*, zebrafish, medaka, stickleback, chicken, mouse and human. The yellow box highlights the clustering of the medaka and stickleback CapZα1 subunits. The pink box highlights the clustering of the CapZα2 subunits. The blue box highlights the separate clustering of the CapZα1 subunits of higher vertebrates. Units at the bottom of the tree indicate the number of substitution events. Boostrap values (an estimate of the reliability of each branch point) were calculated based upon a 1000 bootstrap trials (i.e. the displayed tree was compared 1000 times to random tree constructs) and a random seed of 111 (the default setting). The random seed is a number used to initialize the pseudorandom generator and makes bootstrapping consistent with the Clustal interface.

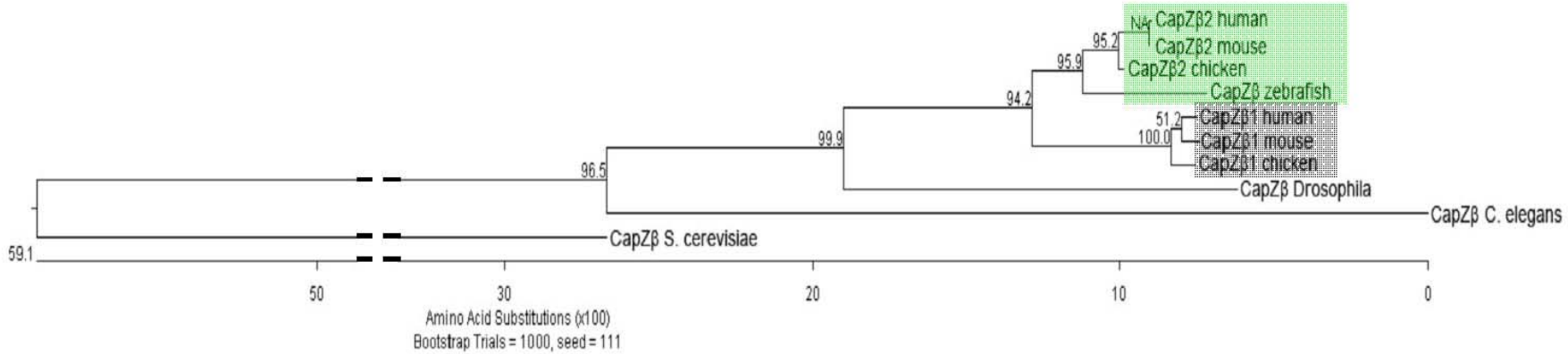

Fig.4.4B. Phylogenetic tree of CapZβ subunits from various species. The Clustal W program was used to align amino acid sequences from yeast (*S. cerevisiae*), worm (*C.elegans*), *Drosophila*, zebrafish, chicken, mouse and human. The green box highlights the clustering of the CapZβ2 subunits and the grey box highlights the clustering of the CapZβ1 subunits. Units at the bottom of the tree indicate the number of substitution events. Boostrap values were calculated based upon a 1000 boot strap trials and a random seed of 111.

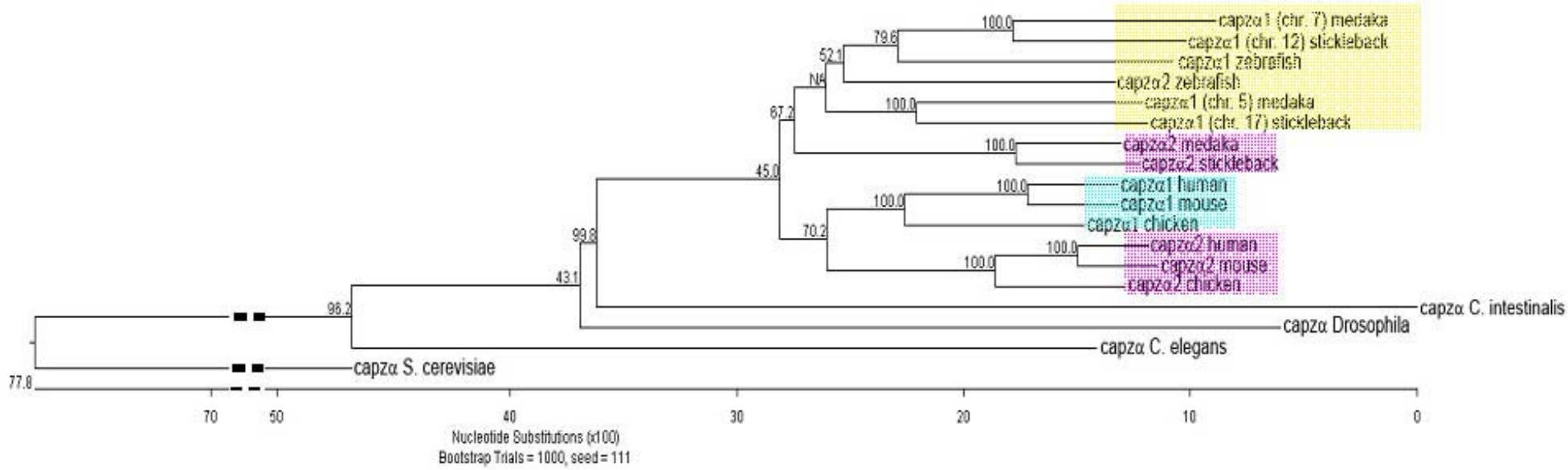

Fig.4.5. Phylogenetic tree using DNA sequence of the α subunits of *capz* from various species. The Clustal W program was used to align DNA sequences from yeast (*S. cerevisiae*), worm (*C. elegans*), *Drosophila*, zebrafish, chicken, mouse and human. Pink and yellow boxes highlight the clustering of the *capzα2* and *capzα1* subunits respectively. The blue box highlights the separate clustering of the capzα1 subunits of higher vertebrates.Units at the bottom of the tree indicate the number of substitution events. Boostrap values were calculated based upon a 1000 bootstrap trials and a random seed of 111.

residues in the corresponding orthologues. It is therefore debatable as to whether these key regions truly signify the difference between the α1 and α2 subunits as the data was based on comparison of only higher vertebrate sequences.

Hart and colleagues (1997b) also compared the 3′ UTR of *capzα1* and *capzα2*, and found that there is approximately 60% and 70% identity for α1 and α2 respectively between chicken, mouse and human. However, when comparing the similarity between the 3′ UTR of α1 and α2, only 32% identity was observed. In zebrafish, the UTR is far less conserved when compared to the other species, and *capzα1* only shares approximately 36% identity with the higher vertebrates (Table 4.1). This finding was also apparent with the 3′ UTR of *capzα2*, and only 35% DNA sequence identity was observed. Therefore, by comparing the 3′ UTR I was still unable to verify that zebrafish *capzα1* is located on chromosome 8.

Another approach commonly used to give an indication of gene orthology between species is to investigate its synteny. Syntenic regions are genetic loci that lie in the same order on a chromosome in different species, indicating that they derive from a common ancestral chromosome. Zebrafish *capzα1* was found to share greater synteny with the regions surrounding *capzα1* in other species (Fig. 4.6). Four common genes were located near *capzα1* in mouse, human and zebrafish: *rho2*, *wnt2bb*, a putative helicase *mov10* and *cttnbp2*. The region surrounding zebrafish *capzα2* only shared *suppressor of tumorigenicity 7* (*st7*) with the mouse and human *capzα2* equivalent region. BLAST comparison of zebrafish *st7* against mouse *st7* and *st7-like isoform 3* (syntenic with *capzα1* in mouse and human) was performed to verify that zebrafish *st7* had been annotated correctly. Zebrafish *st7* shares 81% amino acid identity to mouse *st7* and 69% amino acid identity to mouse *st7-like isoform* 3 indicating that *st7* is indeed syntenic with *capzα2*. Zebrafish *capzα2* therefore does not share any synteny with the region

surrounding *capzα1* in mouse and human and vice versa. The synteny of *capzα1* provides the strongest evidence that zebrafish *capzα1* is located on chromosome 8 and *capzα2* is located on chromosome 6.

Table 4.1. Percentage of DNA sequence identities of zebrafish *capzα1* and *capzα2* 3′ UTRs (700bp) against chicken, mouse and human *capzα1* and *capzα2* 3′ UTRs.

	Chicken	Mouse	Human
capzα1 zebrafish	34.6%	38%	37.1%
capzα2 zebrafish	35.5%	36.1%	35.8%

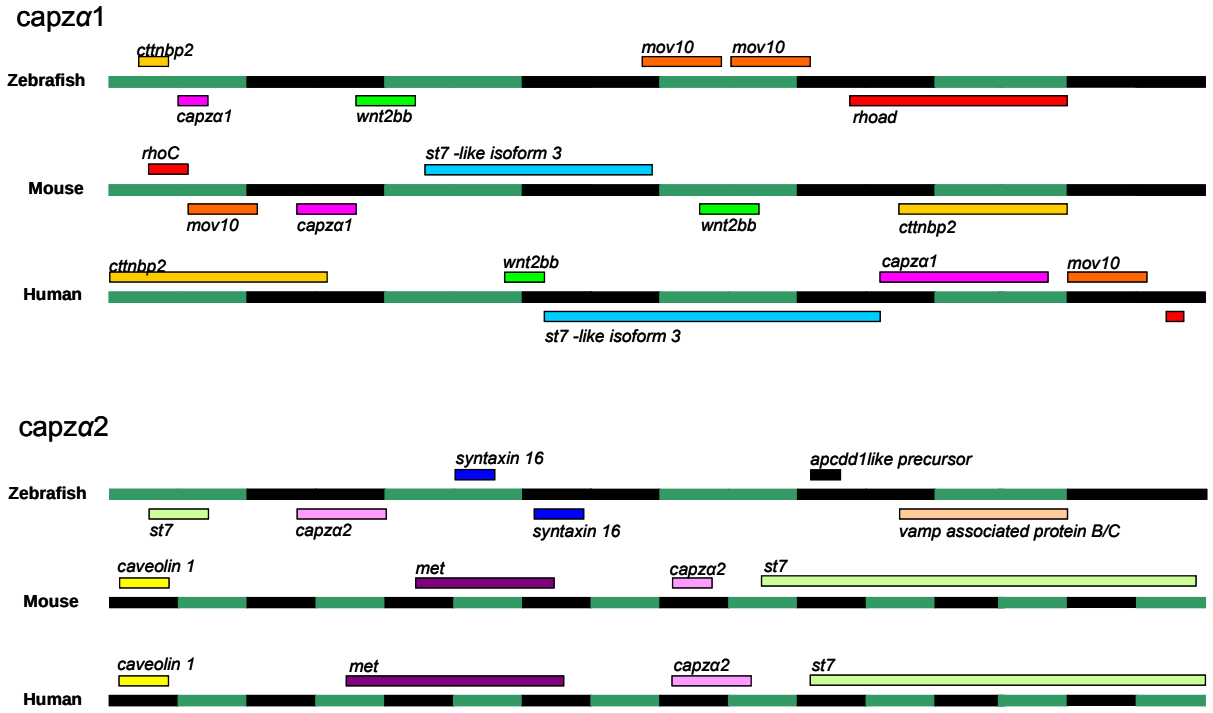

Fig. 4.6. Syntenic regions surrounding *capzα1* and *capzα2* in zebrafish, mouse and human. *mov10* is a putative helicase (moloney leukemia virus), *cttnbp2* is cortactin binding protein 2 N-terminal-like gene, *met* is a proto-oncogene, *apcdd1-like precursor* is adenomatosis polyposis coli down- regulated 1–like protein, *vamp* is vesicle-associated membrane protein and *st7* is suppressor of tumorigenicity-7. Green and black bars represent represent 0.04 Mb.

4.3.2 CapZβ

Isoforms 1 and 2 of CapZβ in chicken, mouse and human differ only in the last 27-31 amino acids and arise from alternative splicing of the last exon (Fig.4.7). Unexpectedly, only one *capzβ* isoform has thus far been identified in zebrafish. Alignments of the zebrafish CapZβ sequence (derived from cDNA sequence Amsterdam et al., 2003) along with the β1 and β2 orthologous isoforms from other species indicate that zebrafish CapZβ is the β2 isoform (Fig. 4.8). Zebrafish CapZβ shares approximately 89% amino acid identity with the orthologous β1 isoforms and approximately 94% identity with the β2 isoforms. Additionally, in zebrafish CapZβ, 20 amino acids out of the last 26 amino acids are identical with the β2 orthologous isoforms, however, only 8 amino acids out of 26 amino acids are identical with the β1 orthologous isoforms. A phylogenetic tree of the alignments also shows that the zebrafish CapZβ sequence clusters with the CapZβ2 orthologues (Fig. 4.4B) and therefore indicates that the annotated zebrafish *capzβ* is in fact *capzβ2*.

In an attempt to detect expression of the *capzβ1* isoform in zebrafish, RT-PCR was performed using primers that amplified the 3′ region of *capzβ* from 18 somite cDNA. Two products that differed in size by 100bp were amplified (Fig. 4.9), which coincided with the size difference between the cDNA of the chicken β1 and β2 isoforms (Schafer et al., 1994), however, cloning and sequencing of the products revealed that only one of these cDNAs encoded the previously identified *capzβ* isoform 2. The other product matched another region of the genome (an rRNA gene on chromosome 4) and may have arisen from a lack of primer specificity. Due to the poor genomic annotation of zebrafish *capzβ*, I was unable to establish whether the exon characteristic of the β1 isoform was encoded in the 3′ region of the gene.

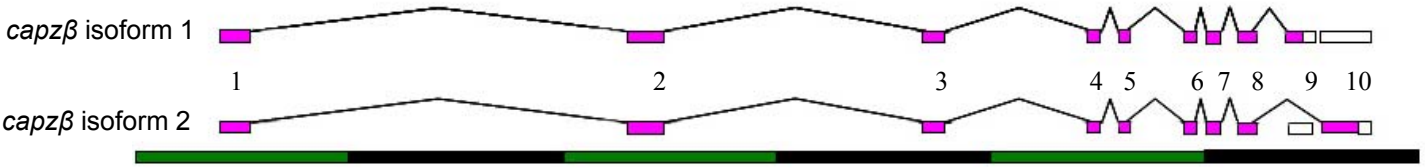

Fig. 4.7. Illustration of *capzβ* exons spliced to form isoforms 1 and 2. Each bar represents 0.04Mb. Isoform 2 skips exon 9 and splices into exon 10 which is encoded in the 3′ UTR of what is transcribed in isoform 1.

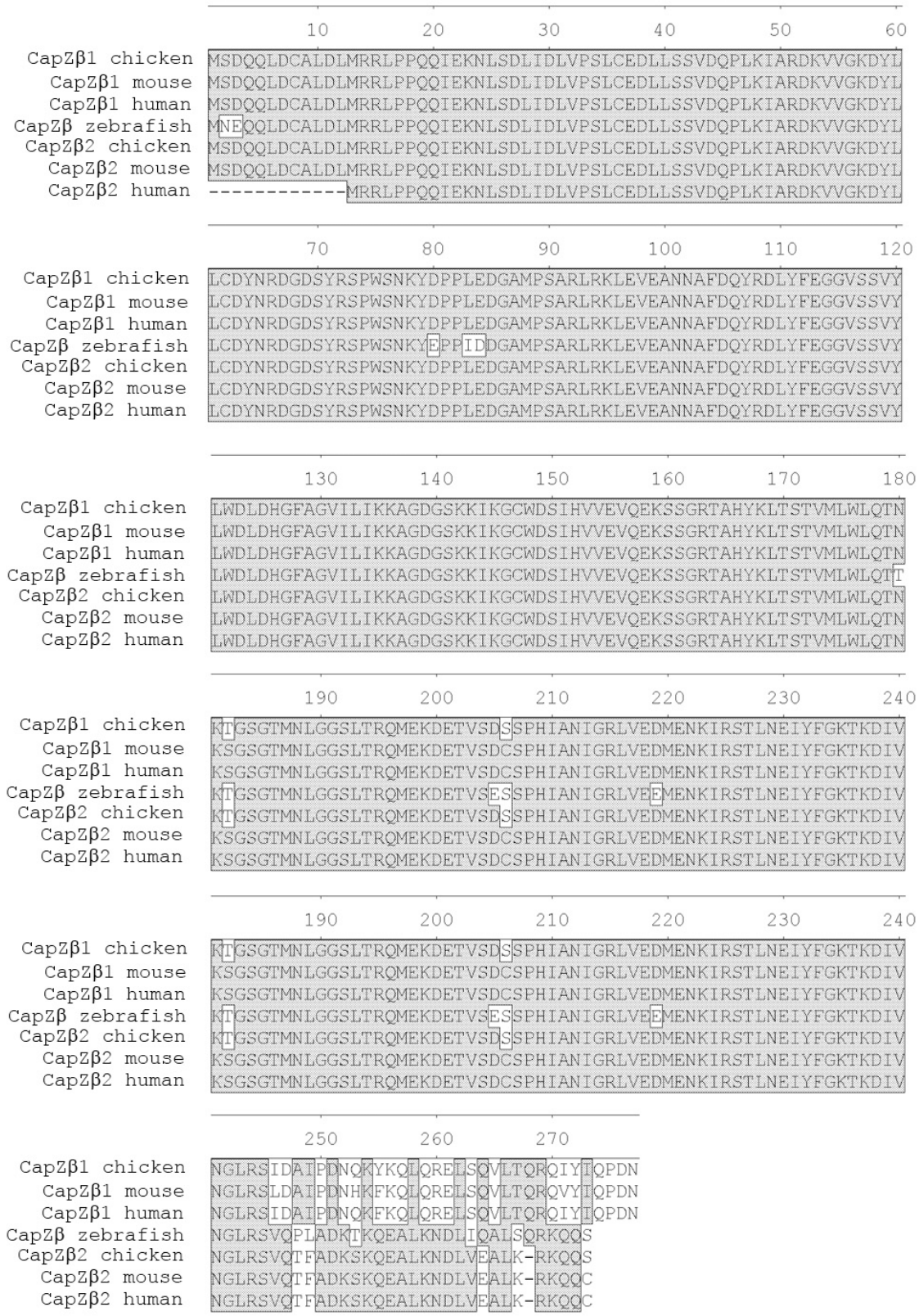

Fig. 4.8. Multiple alignments of CapZβ isoforms 1 and 2 of chicken, mouse and human with the zebrafish CapZβ protein sequence. Amino acids that are identical between the majority of orthologues are shaded.

4.4

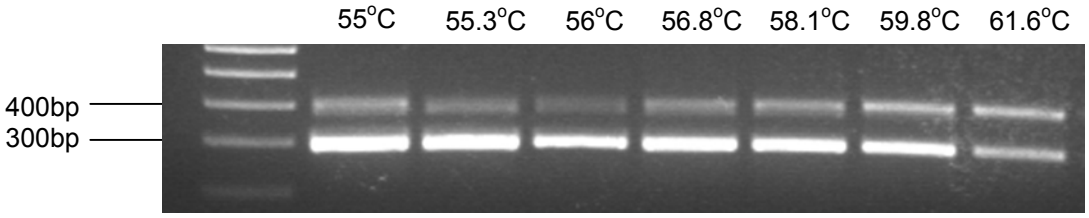

Fig. 4.9. Gel of *capzβ* products from a gradient RT-PCR using 18 somite cDNA.

RNA expression patterns of the *capz* subunits

4.4.1 Probe design

To examine the RNA expression profile of the *capz* subunits during zebrafish embryonic development, labeled antisense RNA probes for *capzα1*, *capzα2* and *capzβ* were constructed. Due to the high sequence similarity between the coding regions of *capzα1* and *capzα2* (80% DNA sequence identity), the probes for these genes were designed to bind predominantly to the more divergent 3′ UTR (Fig. 4.10). The *capzα1* probe targeted just the 3′ UTR of *capzα1* (599bp), and the *capzα2* probe targeted the last 266bp of the coding sequence and 214bp of the 3′ UTR. The region that overlapped between the two probes had low sequence similarity (40 %), therefore the likelihood that the probes would be cross reactive was extremely low. The *capzβ* antisense RNA labeled probe (595bp) was designed to bind to the 5′ region of the coding sequence, beginning at the start site.

4.4.2 The *capzα1* expression pattern

Expression of *capzα1* RNA is first observed very early in development, and is present by the 16-cell stage (Fig. 4.11A), demonstrating that *capzα1* is expressed maternally. At 90% epiboly and 13-15 somites there is ubiquitous expression (Fig. 4.11C-F), however, by 24 hpf stronger expression is detected within the somites, midbrain, hindbrain and the eye (Fig. 4.11G). This expression pattern is also apparent at 48 hpf (Fig. 4.11H), and heart-specific expression is also observed at this stage (Fig. 4.11I).

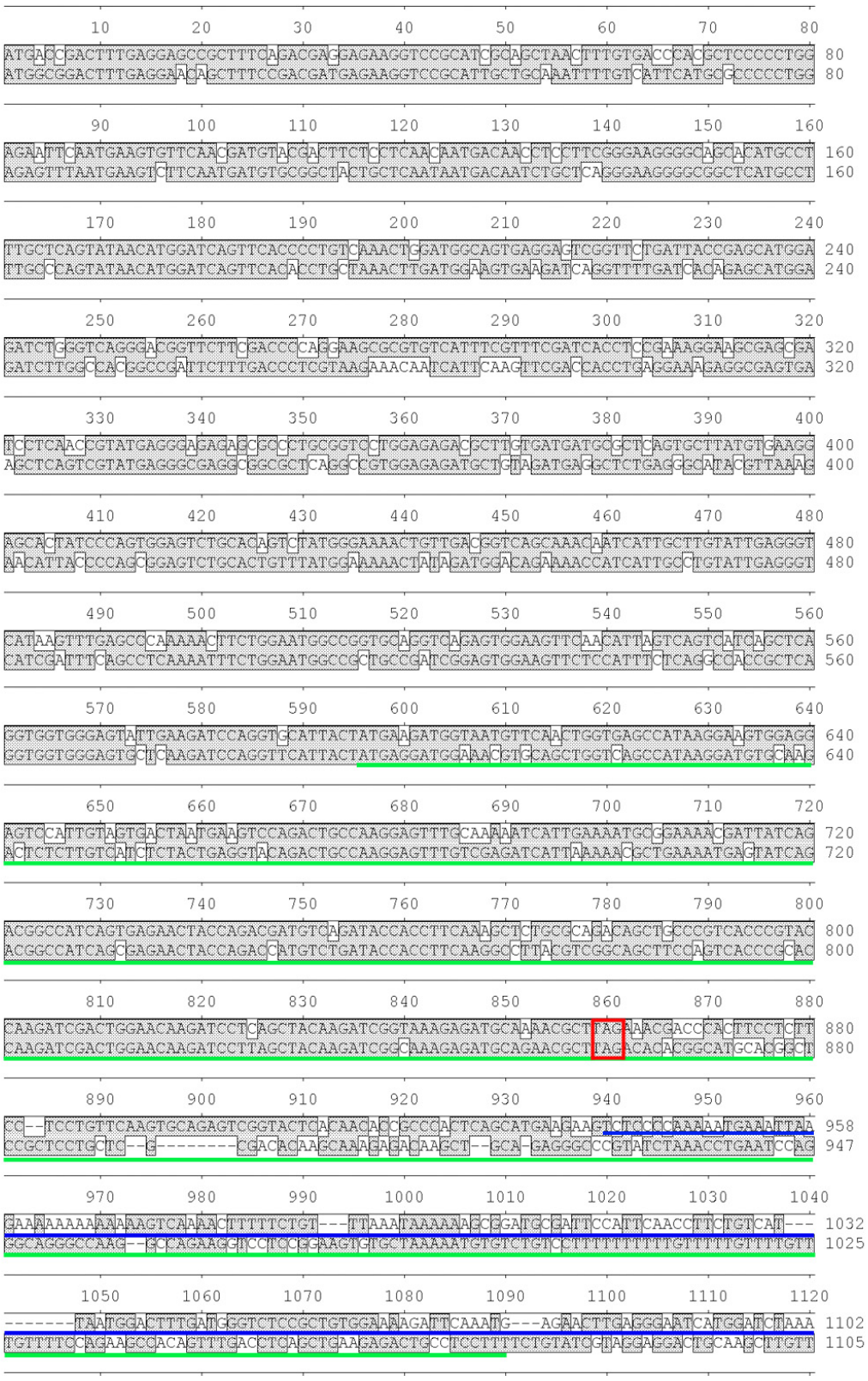

Fig. 4.10. Legend overleaf.

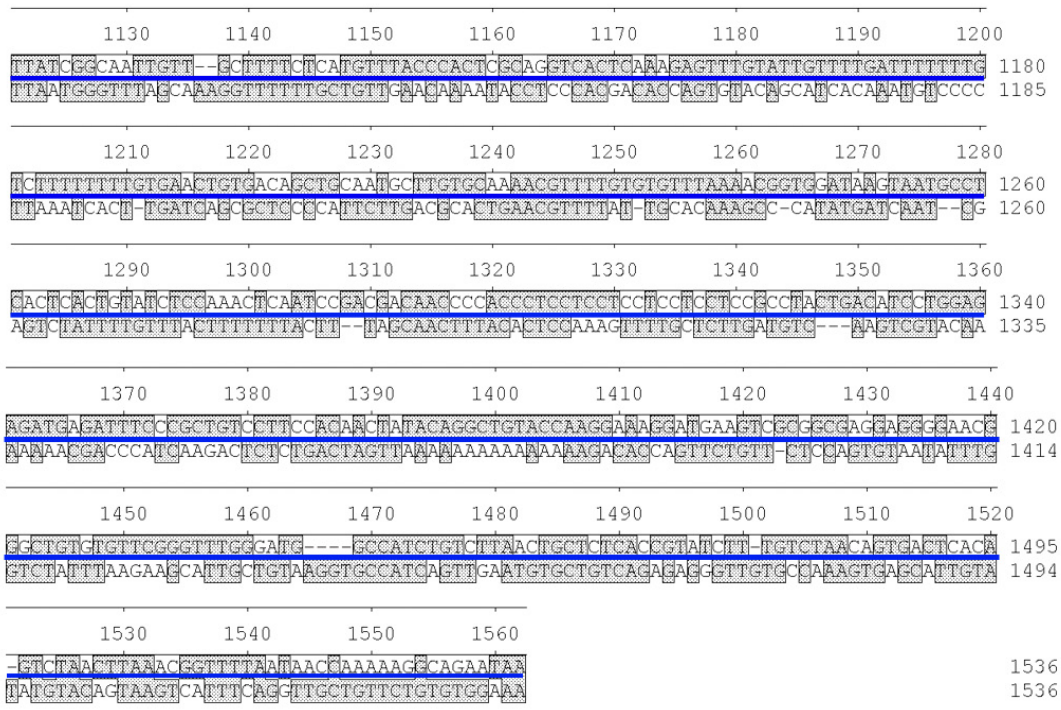

Fig. 4.10. Alignment of *capzα1* and *capzα2* zebrafish cDNA sequence. The *capzα1* RNA *in situ* probe targets the region underlined in blue and the *capzα2 in situ* probe targets the region underlined in green. The *capzα1* RNA *in situ* probe shares 43% sequence identity with *capzα2* and the *capzα2 in situ* probe shares 67% sequence identity with *capzα1*. The stop codon is boxed in red.

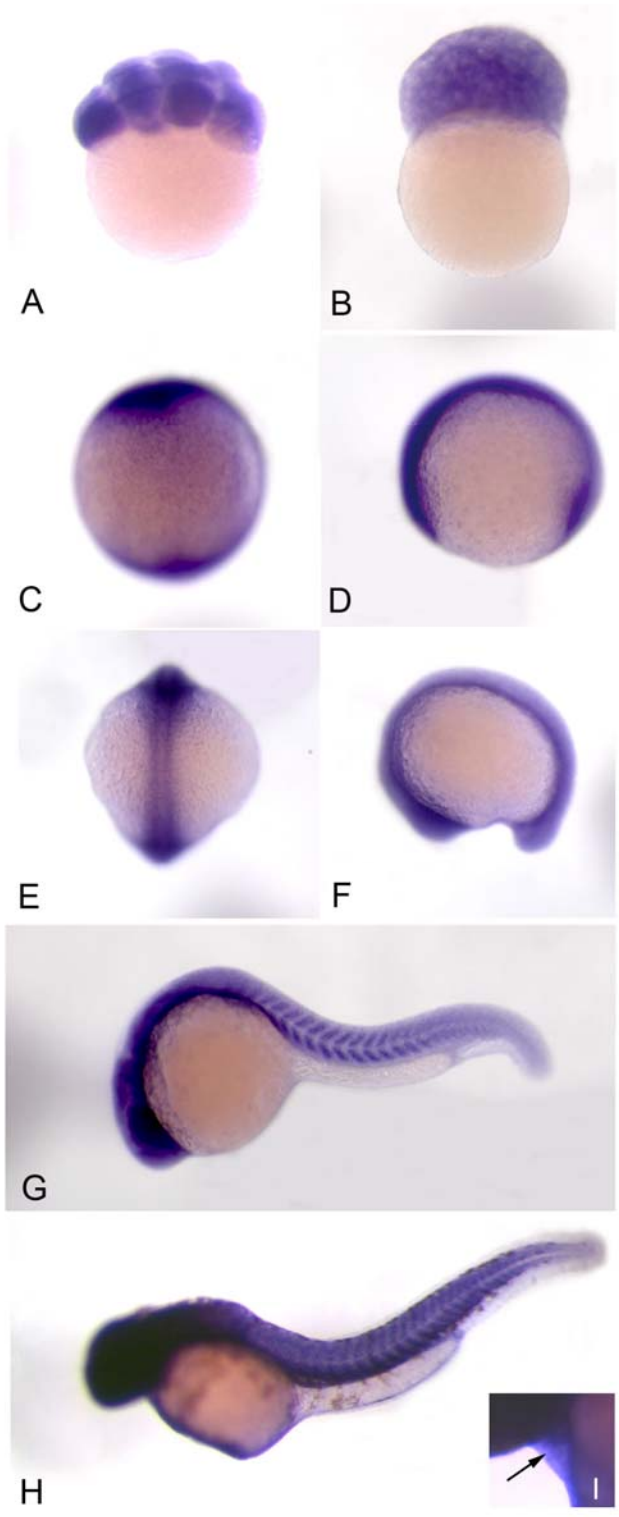

Fig. 4.11. *capzα1* RNA *in situ* expression pattern at different stages of zebrafish embryonic development. A) 16 cell, B) 128 cell, C and D) 90% epiboly, E and F) 13 -15 somites, G) 24 hpf and H) 48 hpf. I) Close up of the heart at 48 hpf. Arrow points to expression in the heart.

4.4.3 The *capzα2* expression pattern

A low level of ubiquitous *capzα2* RNA expression is detected at all the stages of development tested. Like *capzα1*, expression of *capzα2* is first observed at the 16 cell stage (Fig. 4.12A) indicating that *capzα2* is also expressed maternally. Expression is ubiquitous at 90% epiboly and 13-15 somites (Fig. 4.12C-F), and by 24 hpf stronger expression in the midbrain, hindbrain and the eye is detected, however, in the trunk of the embryo expression is ubiquitous but greatly reduced (Fig. 4.12G). This is distinct from the stronger blocks of expression that were observed in the somites with the *capzα1* probe. By 48 hpf the expression pattern remained similar to the 24 hpf embryo (Fig 4.12H) with the addition of clearly detectable staining in the heart (Fig. 4.12I).

4.4.4 The *capzβ* expression pattern

The expression pattern of *capzβ* is very similar to *capzα1*. As with the α subunits *capzβ* RNA is also first expressed maternally and is detected at the 16 cell stage (Fig. 4.13A). At 90% epiboly and 13-15 somites ubiquitous expression is observed (Fig. 4.13C-F), however, by 24 hpf stronger expression is localized to the somites, midbrain, hindbrain and the eye (Fig. 4.13G). This expression pattern continues at 48 hpf (Fig. 4.13H), and expression of *capzβ* is also seen in the heart (Fig. 4.13I).

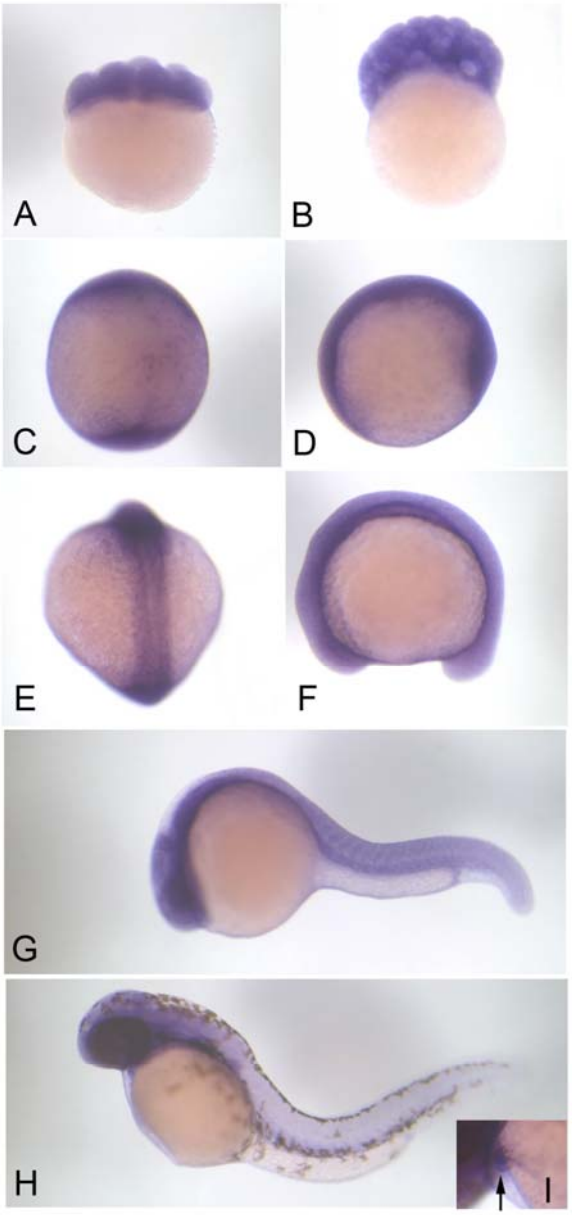

Fig. 4.12. *capzα2* RNA *in situ* expression pattern at different stages of zebrafish development. A) 16 cell, B) 128 cell, C and D) 90% epiboly, E and F) 13 -15 somites, G) 24 hpf and H) 48 hpf. I) Close up of the heart of 48 hpf. Arrow points to expression in the heart.

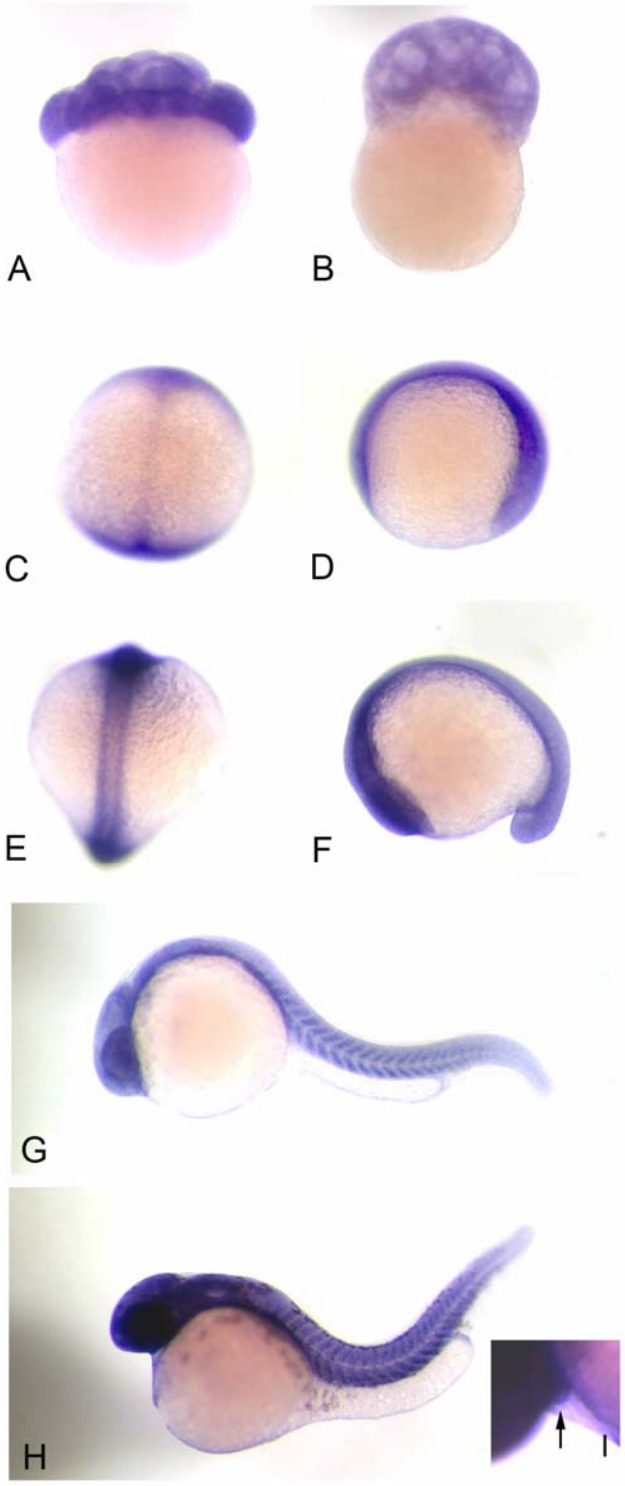

Fig. 4.13. *capz*β RNA *in situ* expression pattern at different stages of zebrafish development. A) 16 cell, B) 128 cell, C and D) 90% epiboly, E and F) 13-15 somites, G) 24 hpf and H) 48hpf. I) Close up of the heart at 48 hpf. Arrow indicates expression in the heart.

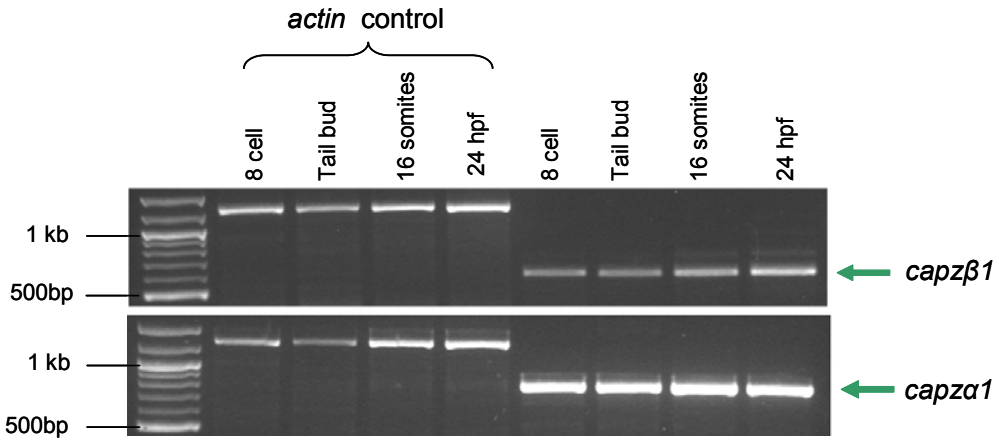

Fig. 4.14. Gel of *capzα1* and *capzβ* RT-PCR products amplified from cDNA of 8 cell, tail bud, 16 somites and 24 hpf embryos. Actin was also amplified as a control. Primers are shown in Table 2 of the appendix.

4.4.5 Expression of *capzα1* and *capzβ* detected by RT-PCR

To confirm that *capzα1* and *capzβ* are expressed throughout the early stages of development RT-PCR was performed on RNA extracted from 8 cell, tail bud, 16 somites and 24 hpf embryos (Fig. 4.14). RT-PCR products were amplified from both genes at all stages, confirming the early expression of *capzα1* and *capzβ* indicated by *in situ* hybridizations.

4.5 Morphology of the *sne* mutant

To investigate how the mutation in *capzα1* affects muscle structure and function, the morphology of *sne* mutant skeletal muscle was examined. This following section describes the skeletal muscle phenotype of *sne* mutants by using light microscopy, immunostaining and TEM techniques.

4.5.1 Gross morphology observed by light microscopy

The motility defect in the *sne* mutant is apparent by 4 dpf, as embryos are unable to respond to a stimulus as quickly as wild type embryos. Additionally, the swim bladder fails to inflate and wavy muscle fibres can be detected by differential interference contrast (DIC) microscopy in the mutants (Fig. 4.15). Mutant embryos die soon after transfer to the fish facility, most likely as a result of being unable to find food, due to their inability to swim properly. In the original description of this mutation reduced birefringence was seen in the muscle of *sne* mutants (Granato et al., 1996). Birefringence is the ability of muscle to rotate polarized light due to its highly ordered structure and is used to identify any defects in muscle organization.

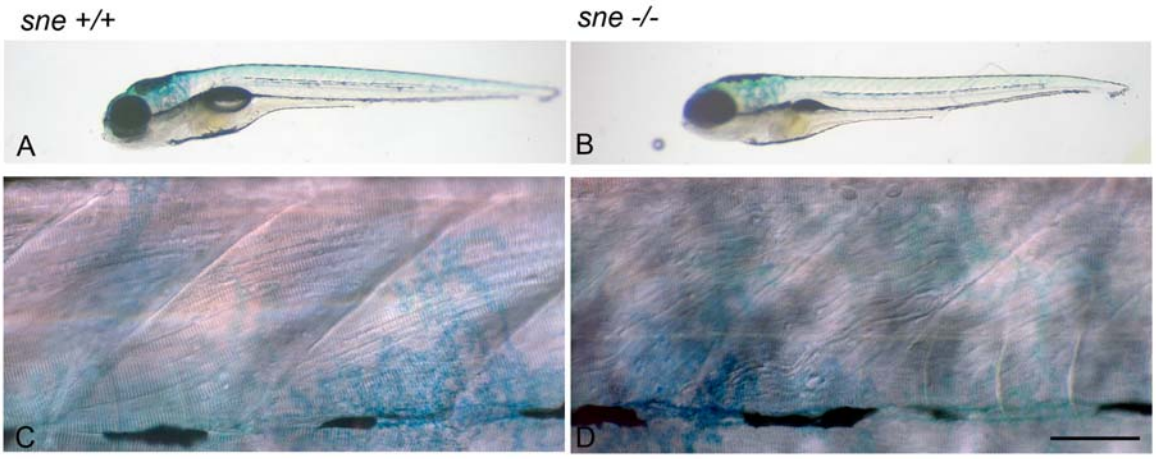

Fig.4.15. Live images of *sne* mutant and wild-type sibling 5 dpf embryos. Wild-type sibling (A and C) and *sne* mutant (B and D) images of the whole embryo (A and B) and the skeletal muscle under DIC microscopy (Cand D). The scale bar for C and D =100μm.

4.5.2 Immunostaining of F-actin and α-actinin in *sne* mutants

Closer inspection of the skeletal muscle was achieved by staining of the actin filaments and Z-lines. Phalloidin conjugated to FITC was used to detect the actin filaments. Phalloidin (a toxin that was originally isolated from the *Amanita phalloides* mushroom) binds filamentous actin (F-actin) at the junction between each monomeric actin subunit (Barden et al., 1987; Faulstich et al., 1993; Steinmetz et al., 1998). In the *sne* mutants both slow and fast F-actin are detected, however, fewer muscle fibres are observed in mutant embryos than in their wild-type siblings. Moreover, the fibres are wavy and accumulations of actin filament are observed at myoseptum boundaries (Fig. 4.16A and B). α-Actinin staining reveals that Z-lines are formed in *sne* mutant embryos, however, the Z-lines are not aligned laterally between myofibrils and the fibrils appear to be detached from the myoseptum (Fig. 4.16C and D). α-Actinin also accumulates at the myoseptum boundaries.

At 2 dpf Mendelian ratios of mutants were observed by scoring the morphology of the actin filament using phalloidin staining. Three out of ten embryos derived from a heterozygous cross had detectably abnormal 'wavy' myofibre organization (Fig. 4.17). Although this phenotype is less pronounced than at 5 dpf, it suggests that the muscle defect in the *sne* mutants worsens over time. However, greater numbers and genotyping of fixed embryos would be necessary to verify this result fully.

4.5.3 The expression levels of *capzα1* and *capzβ* are not reduced in the *sne* mutant

It has been speculated that the α and β CapZ subunits regulate each other's expression, therefore RNA levels of *capzα1* and *capzβ* were examined in 24 hpf *sne* mutant and wild-type sibling embryos by performing RNA *in situ* hybridizations. Mutants and wild-type siblings are

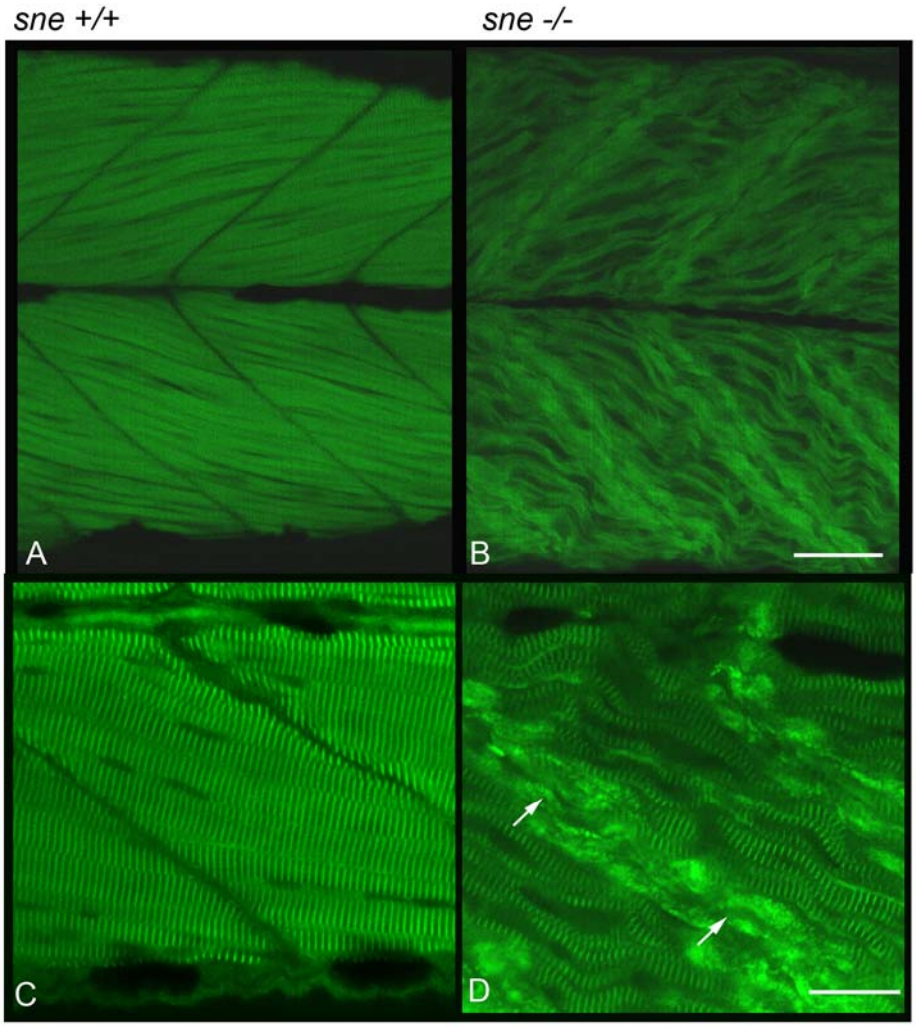

Fig. 4.16. Phalloidin (A and B) and α-actinin staining (C and D) of *sne* wild-type sibling (A and C) and mutant (B and D) at 5 dpf. Arrows indicate accumulations of α-actinin adjacent to the myoseptum. The scale bar for A and B = 44.36μm and for C and D =22.18μm.

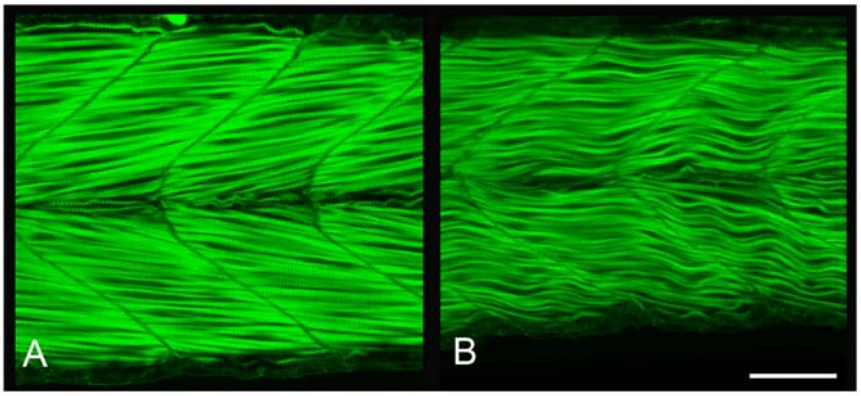

Fig. 4.17. Phallodin staining of 2 dpf *sne* wild-type sibling and mutant embryos. A) Wild-type sibling, B) possible mutant embryo, note the slightly wavy myofibres.Scale bar = 44.36μm.

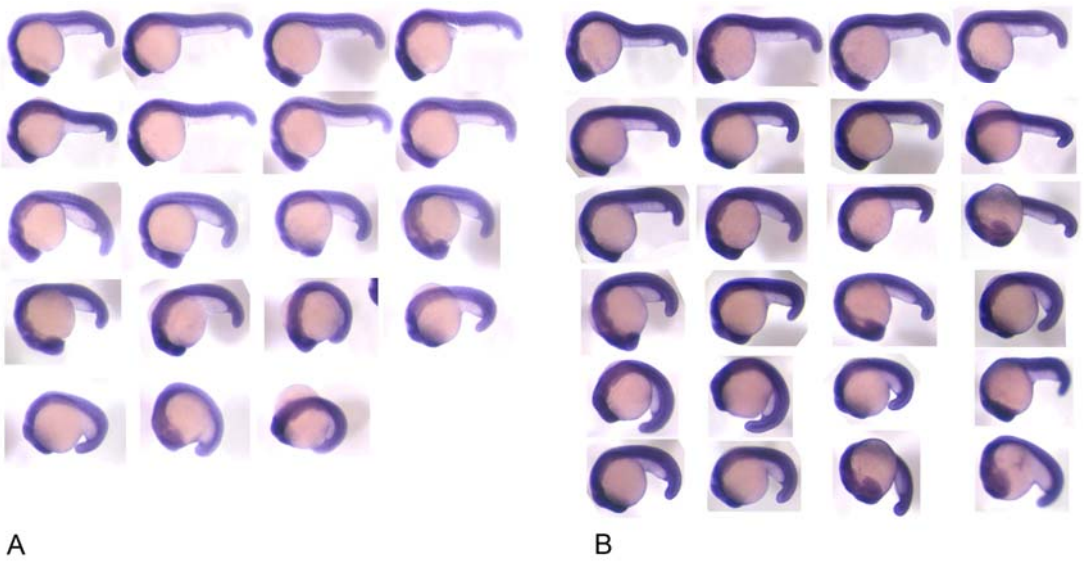

Fig. 4.18. RNA *in situ* expression pattern of A) *capzα1*and B) *capz*β in 24hpf *sne* mutant and wild-type sibling embryos.

not distinguishable at this stage, so 19 and 25 embryos from a heterozygous cross were hybridized with *capzα1* and *capzβ* RNA probes respectively. Differences in levels of *capzα1* and *capzβ* RNA expression were not detected in any of the embryos tested (Fig. 4.18) and therefore indicate that RNA levels of each gene are not affected in this mutant. As *capzα1* RNA appears to be expressed at normal levels in the mutant it also suggests that the mutation does not affect transcription levels of *capzα1*, nor induces RNA degradation of the transcript. However, as this experiment is only semi-quantitative, real time RT-PCR will be required to verify this finding.

4.5.4 Immunostaining of CapZα1 in *sne* mutants

To determine whether mutant *capzα1* transcript (observed from the *in situ* hybridization experiments and the RT-PCR in chapter 3) is translated, *sne* mutant and wild-type sibling embryos were immunostained with a polyclonal antibody raised in chicken against recombinant human CapZα1 (Abcam). In the skeletal muscle of day 5 wild type zebrafish embryos CapZα1 localizes to Z-lines, as determined by co-immunostaining with α-actinin (Fig. 4.19A-C). Additionally, CapZα1 is also localized to the myoseptum. In the mutants CapZα1 is detected, however it is mis-localized and accumulates adjacent to the myoseptum. Intriguingly, this mis-localization largely associates with the aberrant accumulation of α–actinin at the myoseptum (Fig. 4.19D-F).

4.5.5 Transmission Electron Microscopy (TEM)

TEM of *sne* mutant skeletal muscle (performed by David Goulding) show that thick and thin filaments incorporate into the sarcomere (Fig. 4.20). Distinct M-bands, I-bands and A-bands are still observed in most sarcomeres, however, the I-bands appear larger than in the wild type embryos and the thin filaments seem to be splayed at the Z-line within this region (Fig. 4.20B). In

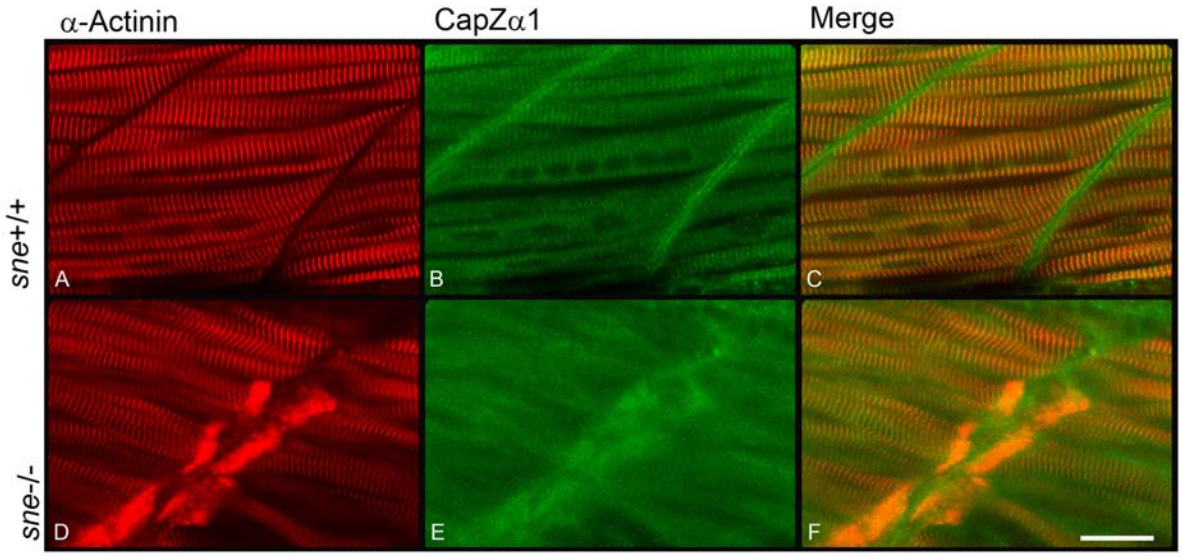

Fig. 4.19. Co-immunostaining of CapZα1 and α-actinin. *sne* wild-type sibling (A-C) and mutant (D-F) 5dpf embryos stained with the α-actinin (A and D) and CapZα1 antibody (B and E). The merge of both these stainings is shown in C and F. Scale bar = 22.18μm.

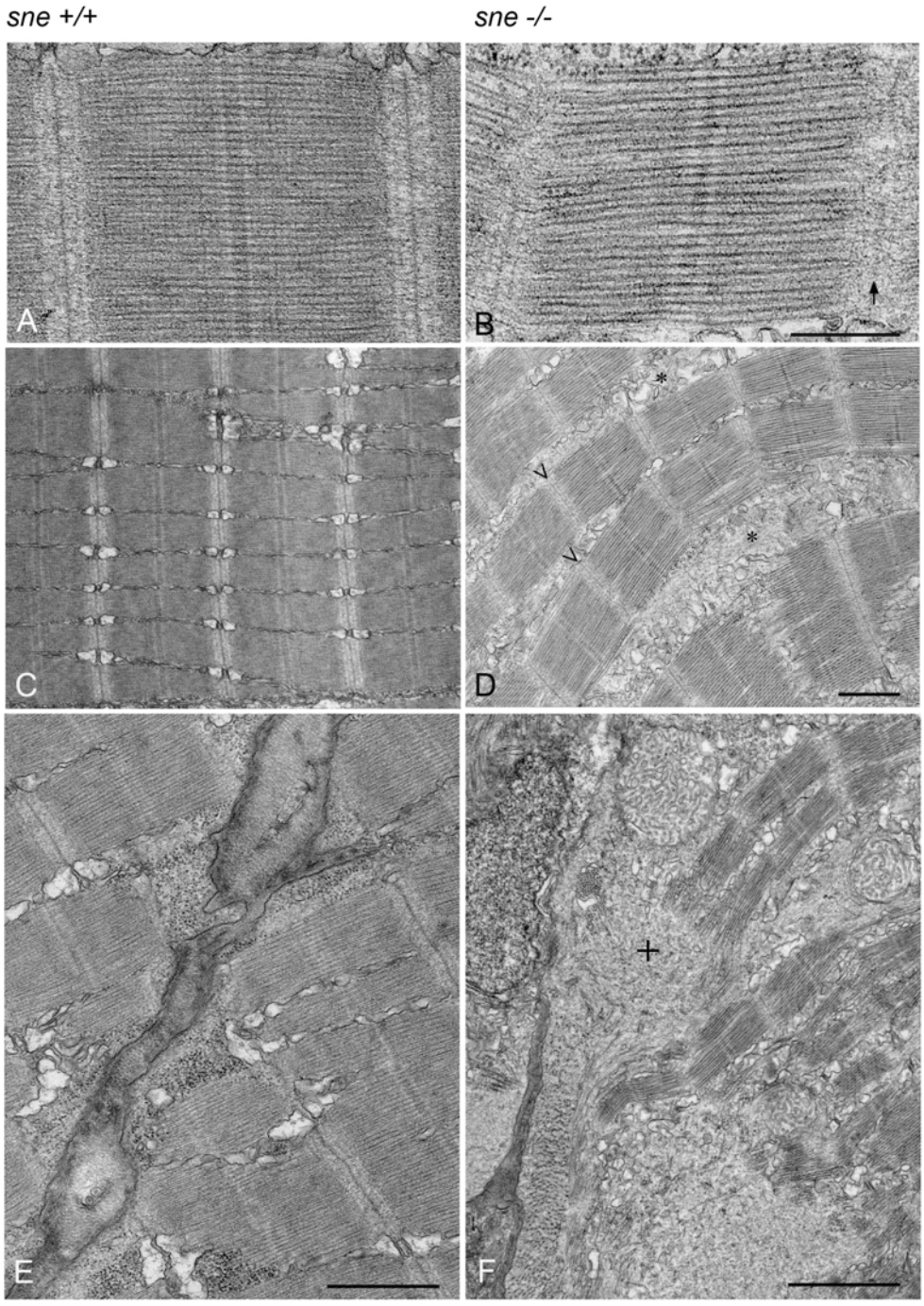

Fig.4.20. TEM of skeletal muscle in *sne* wild-type sibling (A, C and E) and mutant (B, D and F) 5 dpf embryos. Arrow in B indicates the remnants of Z-line in the mutant. Arrowheads in D point to the misalignment of Z-lines between myofibrils and asterisks indicate the accumulation of sarcoplasmic reticulum. Cross in F indicates the accumulations of protein adjacent to the myoseptum boundary. Scale bar for A and B=660nm, C and D=1364nm, E=1480nm and F=2960nm.

many sarcomeres the Z-line is not well defined compared to wild-type embryos and appears much more diffuse. Additionally, in some sarcomeres the Z-lines have partially disintegrated. In some regions the Z-lines are not aligned between myofibrils and sarcoplasmic reticulum has accumulated between myofibrils (Fig. 4.20D). The wavy myofibrils that were observed by immunostaining are also detected by TEM and these images suggest that the myofibrils are separating from each other and breaking apart. The myosepta in the *sne* mutant are also less distinct than the wild-type embryos and sarcomeres that had attached directly to the myoseptum were not observed. Instead, un-incorporated protein aggregates, most likely to be F-actin and/or α-actinin (which were observed in the immunostaining) accumulate adjacent to the myoseptum (Fig. 4.20F).

To determine whether sarcomere size is affected in the *sne* mutants, the length of each sarcomere was measured and compared to wild-type sarcomere length. The sarcomeres were measured from the TEM images using Zeiss Axiovision Rel. 4.5 software. Sixty nine and seventy sarcomeres from one wild-type sibling and one mutant 5 dpf embryo were measured respectively. Surprisingly, the *sne* mutants have significantly shorter sarcomeres compared to their wild-type siblings, and the confidence interval (99%) calculated for wild-type (2738nm +/- 178nm) and mutant (1747 nm +/- 180.6nm) sarcomere lengths were not overlapping. The box and whisker plot shown in Fig. 4.21 indicates that the range of sarcomere length in both the mutant and the wild-type is actually very small (wild-type: 2640.6nm - 2902.2 nm, mutant: 1614.4nm - 1887.9nm). However, additional measurements of sarcomere widths from a greater number of samples will need to be performed to substantiate this finding.

The TEM analysis on the *sne* mutants has revealed that although the main components of the sarcomere are present there remain significant defects in muscle ultrastructure; in particular in

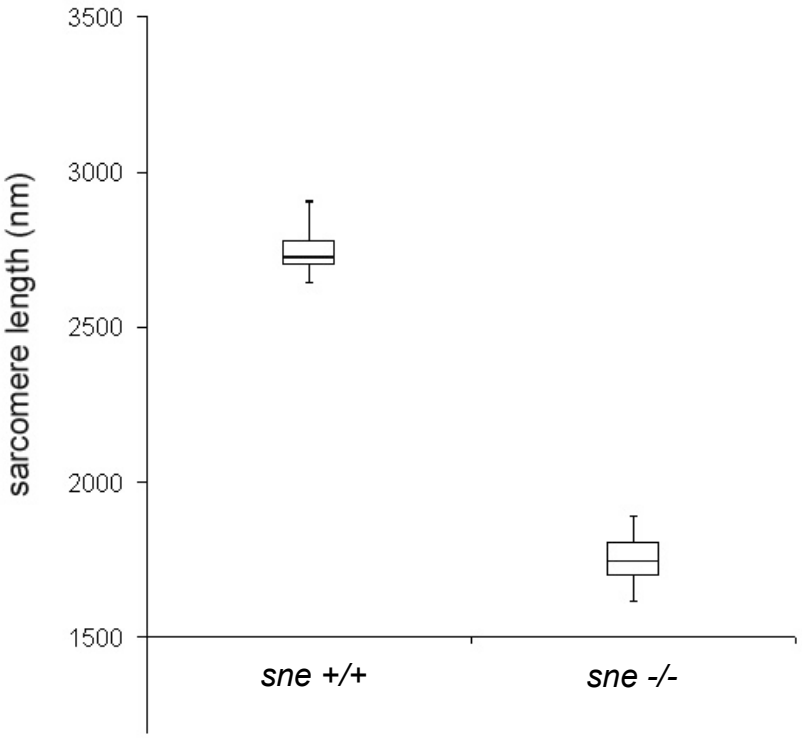

Fig. 4.21. Box and whisker plot of 5 dpf *sne* wild-type sibling and mutant sarcomere lengths. The median is indicated as the line through the centre of each box.

sarcomere length, Z-line integrity, proper myofibrillar organization, attachment and tethering to the myoseptum.

4.6 The *sne* phenotype is ameliorated by decreased muscle usage

To determine whether the *sne* mutant phenotype was enhanced by excessive muscle use, 2 day old sibling and mutant embryos (40) were grown in either just Egg water, Egg water with 0.005% tricaine or Egg water with 0.6% methyl cellulose for 3 days. Tricaine (an anesthetic) inhibits the embryos from freely swimming in the dish, however, they still twitch slightly when touched. The methyl cellulose increases the viscosity of the Egg water, thereby requiring the embryos to place greater strain on their muscles when swimming. At 5 dpf, mutant embryos in methyl cellulose are discernible from wild-type siblings. Conversely, for the embryos that were exposed to tricaine, it was difficult to distinguish mutants from wild-type siblings. Therefore mutants had to be scored using DIC microscopy to visualize the wavy myofibre phenotype. Follow-up phalloidin staining of the identified mutants, shows that the mutant embryos exposed to tricaine have straighter fibres compared to those embryos left in methyl cellulose or in normal media (Fig. 4.22). The methyl cellulose treatment did not enhance the wavy phenotype, which suggests that normal movement in water will produce the wavy myofibres. These experiments demonstrate that the *sne* phenotype is exacerbated by muscle use and they also indicate that CapZ plays an important role in maintaining the integrity of the myofibrillar architecture.

4.7 Discussion

Two *capzα* isoforms were found in the zebrafish genome that share high homology and identity in their DNA and protein sequences. Various comparison tools were utilized to examine

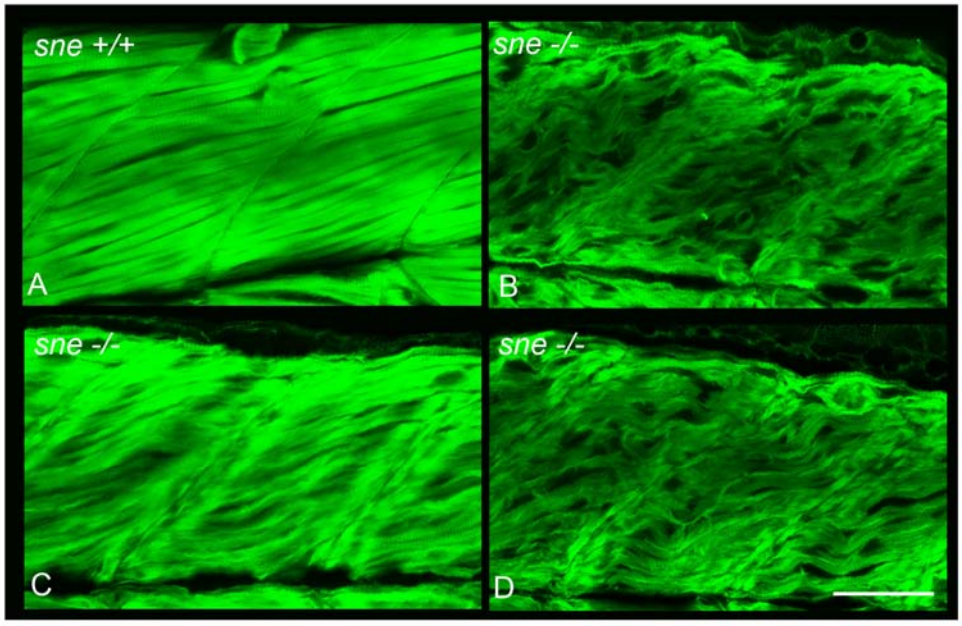

Fig. 4.22. Phalloidin staining of 5dpf *sne* wild-type sibling and mutant embryos grown in Egg water with the addition of methyl cellulose (0.6%) or tricaine (0.005%) from day 2 to day 5 of development. A) Wild-type sibling embryo grown in tricaine B) *sne* mutant embryo grown in Egg water only, C) *sne* mutant embryo grown in tricaine and D) *sne* mutant embryo grown in methyl cellulose. Scale bar= 44.36μm.

homology between zebrafish *capzα* subunits and those of other species to establish conclusively the nomenclature of the isoforms in zebrafish. Synteny proved to be the major deciding element in identifying that *capzα1* in zebrafish was indeed located on chromosome 8; the site of the *sne* locus.

The high amino acid sequence identity shared between the two α isoforms raises the possibility that these proteins may be partially redundant in zebrafish. Indeed, the RNA *in situ* expression pattern of *capzα1* and *capzα2* is ubiquitous until 24 hpf, and thus supports the hypothesis that the α subunits may have overlapping functions in the early stages of development. However, by 24 hpf the *capzα1* and *capzβ* expression patterns become stronger in the somites, while the expression pattern for *capzα2* becomes weaker throughout the trunk of the embryo. The differences in staining pattern between the α subunits in the later stages of development could therefore suggest that the α1 subunit predominantly functions in skeletal muscle while the α2 subunit functions in non-muscle cells. Studies performed by Shafer and colleagues in 1994 found that the β subunits are differentially localized in cardiomyocytes and striated muscle cells (the β1 subunit localized to Z-lines and the β2 subunit localized to the intercalated disc and cell-cell junctions), and are therefore thought to have distinct functions *in vivo* (Hart and Cooper, 1999). This feature may also be shared by the α subunits and localization studies of CapZα1 and CapZα2 will no doubt assist in determining whether the α subunits also have non-redundant functions in muscle tissues. As yet it is unclear whether each α subunit is able to bind to more than one β subunit *in vivo*. If this can be proved then one could speculate that the dimerization of different subunit combinations enables CapZ to take on different functions. It is evident that further in-depth analysis is required to fully determine the function of the α subunits and their interactions with the CapZβ isoforms.

A fully functional CapZ protein requires the dimerization of the α subunit with the β subunit. In chicken, mouse and human at least two isoforms of *capzβ* exist, however, in zebrafish only one *capzβ* isoform has been identified. Comparison of the zebrafish CapZβ with its orthologues indicates that it has greater similarity to the β2 isoform than the β1 isoform. RT-PCR was unsuccessful in establishing whether the capzβ1 isoform is also expressed in zebrafish embryos, however, it seems likely that a β1 isoform would exist in zebrafish as two α1 isoforms have been identified. Additionally, the β1 isoform has been reported to be the predominant isoform expressed in muscle, while the β2 isoform is predominantly expressed in non-muscle tissues (Hart et al., 1997b; Schafer et al., 1994). Further investigation into whether a β1 isoform is expressed in zebrafish by genomic re-sequencing of *capzβ* is required to determine whether a second subunit is also encoded in the zebrafish genome.

The most striking morphological feature of the *sne* mutants are the undulating wavy muscle fibres, which are clearly visible following immunostaining of actin filaments and Z-lines. These initial results reveal that F-actin and α-actinin are partly able to localize to the correct regions within skeletal muscle, however, unincorporated accumulations of both these elements were observed adjacent to the myoseptum. TEM images of skeletal muscle in *sne* mutants also reveal that although most of the sarcomeric components are formed, the Z-lines appear to be disintegrating and the highly ordered architecture of the myofibrils and their attachment to the myosepta are lost. The length of each sarcomere in mutants was also shorter than in wild-type siblings. Additionally, inhibition of movement of mutant embryos by anaesthetizing them in tricaine partially rescued the wavy muscle phenotype observed in the *sne* mutant. The phenotypic analysis of this mutant therefore strongly suggests that the mutation in *capZα1* results in the loss of muscle stability and integrity.

No discernible differences in the RNA expression levels of *capzα1* were observed between 24 hpf *sne* sibling and mutant embryos, which suggests that the mutation does not result in RNA degradation of the mis-spliced *capzα1* products, although it is noted that *in situ* hybridizations only give a semi-quantitative view of expression levels. Notably, wholemount antibody staining with a CapZα1 polyclonal antibody supported the RNA *in situ* hybridization results, and revealed that a mutant form of CapZα1 was translated in the *sne* mutants. However, the striated staining pattern in skeletal muscle, characteristic of localization to the Z-line was not observed. Instead, CapZα1 was mis-localized and had aggregated in clumps adjacent to the myoseptum. Intriguingly, the aberrantly localized CapZα1 co-localized with accumulations of α-actinin, also found adjacent to the myoseptum in the mutants. This result suggests that although the mis-spliced transcripts of *capzα1* are translated they are unable to localize to the Z-line, therefore in terms of participating in capping the barbed end of the thin filament within the sarcomere, they are likely to be non-functional. The main questions arising from these experiments are: 1) To what extent is the function of the mis-spliced CapZα1 isoforms deteriorated? E.g. can they still bind to the β subunit? 2) Which mis-spliced transcripts are translated? 3) Is the α2 subunit capable of compensating for the lack of a fully functional CapZα1? In the following chapter I attempt to address these questions by MO and Western analysis.

The overall findings of the examination of the *sne* mutant phenotype are consistent with a model where muscle differentiation and sarcomere assembly does take place in these mutants, however, the loss of functional CapZ destabilizes the link between the actin filament and the Z-line, and as the muscle starts to function the connection is no longer strong enough to endure the continual force placed on the sarcomere by the sliding of the filaments during muscle contraction. Thus the sarcomeric structure gradually disintegrates and induces destabilization of the myofibrillar structure, resulting in wavy myofibres and misaligned Z-lines observed in the *sne*

mutant. These results suggest that CapZ is important in the maintenance of myofibrillar organization, enabling sarcomeres to withstand the pressure applied during muscle contraction.

The subunits of CapZ are highly conserved in vertebrates and undoubtedly play important roles in development. The phenotypic analysis of the *sne* mutant indicates that CapZ is integral to the maintenance of skeletal muscle structure.